Anatomically constrained CT image translation for heterogeneous blood vessel segmentation

Giammarco LA BARBERA[1]
Haithem BOUSSAID[6,2]
Francesco MASO[1]
Sabine SARNACKI[3,4]
Laurence ROUET[2]
Pietro GORI[1]
Isabelle BLOCH[5,1,3]

1 - LTCI,Télécom Paris, Institut Polytechnique de Paris, France;
2 - Philips Research Paris, Suresnes, France;
3 - IMAG2, Institut Imagine, Université Paris Cité, France;
4 - Université Paris Cité, Chirurgie Pédiatrique Viscérale et Urologique, Hôpital Necker Enfants-Malades, APHP, France;
5 - Sorbonne Université, CNRS, LIP6, Paris, France.
6 - Technology Innovation Institute Abu Dhabi, UAE

INTRODUCTION

- Difficulty in constrast-enhanced Computed Tomography (ceCT) image segmentation → Heterogeneity in contrast.
- Combined use of ceCT and contrast-free (CT) CT images can improve the segmentation performances [1]
  PROBLEM: clinicians often acquire only one CT modality. → SOLUTION: unsupervised generative models.
- Difficulty in image-to-image translation with unpaired medical data [2] → Lack of anatomical coherence.
- Exploiting approximately common anatomy between subjects can mitigate this limitation (PBS method) [3].
  PROBLEM : in the abdominal region, the different sizes and lengths of the organs must be taken into account.

PROPOSED METHOD

- To address these issues, we propose an extension of the **CycleGAN** [4] which includes:

(i) the use of Self-Supervised Body Regressor [5], **SSBR**), **to better select anatomically-paired slices**;

(ii) the use of the SSBR score as an auxiliary classifier [6] adding an extra loss function (**L_{ACL}**) to the generator training, **to reinforce the anatomical coherence.**

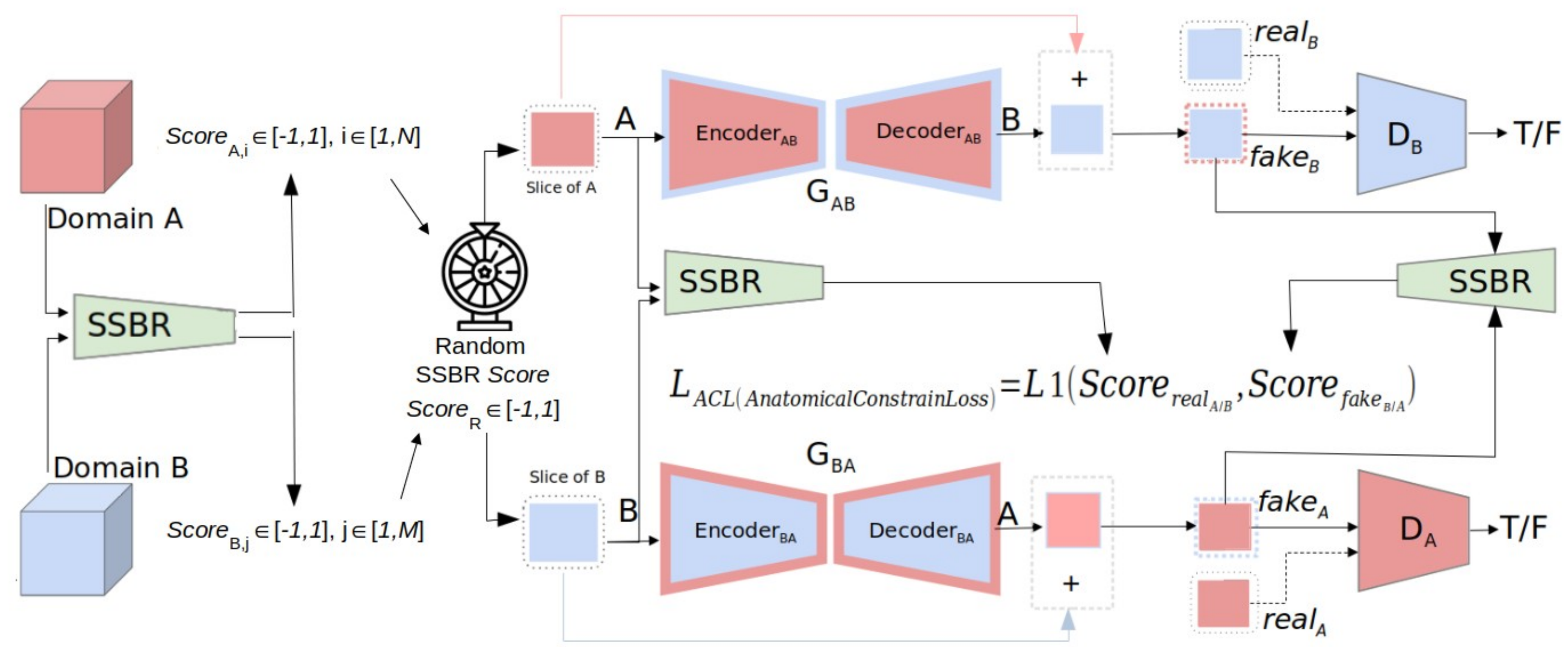

- **SSBR** is trained via the optimization of three loss functions that do not require annotated anatomical labels, to find the scores $Score_{k,p}$:

$$L_{order} = -\sum_{k=1}^{K}\sum_{p=1}^{P-1}\log(h(Score_{k,p+1} - Score_{k,p})) \qquad L_{norm} = \sum_{k=1}^{K}(f(Score_{k,1}+1) + f(Score_{k,P}-1)) \qquad L_{anat} = \sum_{k=1}^{K}\sum_{p=1}^{P-1} f(\Delta^{BM}_{k,p+1} - \Delta_{k,p+1})$$

$Score_{k,p}$ is the SSBR output for slice p of CT volume k; h = sigmoid activation function; f = smoothed L1 norm;
K = number of CT volumes in the mini-batch; P = number of slices in each volume; BM = binary mask.

$$\text{with} \begin{cases} \Delta^{BM}_{k,p} = 1 - \dfrac{|BM_{k,p} \cap BM_{k,p-1}|}{|BM_{k,p-1}|} \\ \Delta_{k,p} = Score_{k,p} - Score_{k,p-1} \end{cases}$$

RESULTS

- **Unpaired training and qualitative results -** public databases of healthy patiens from TCIA [7] of 82 abdominal images for each domain (72 for training, 10 for test)

Evaluation of various existing methods [2,3,4,8] to find the best one (G: generator; D: discriminator)

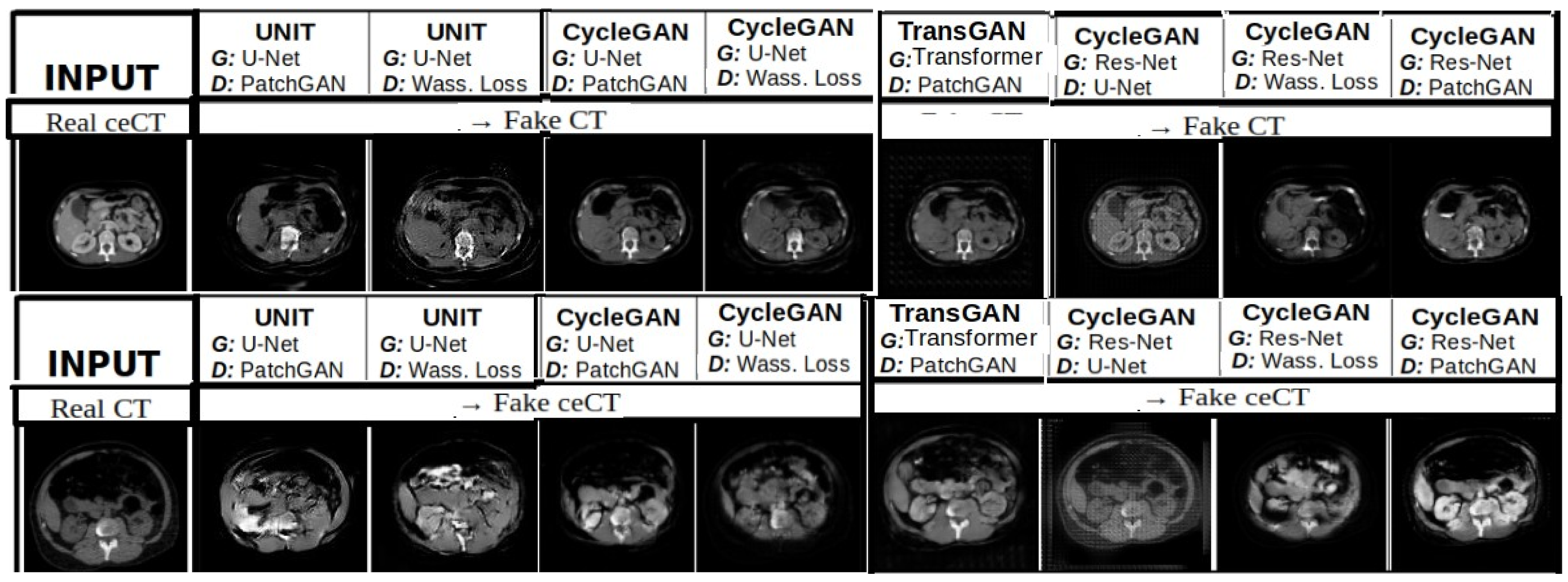

Application of our proposals to the best method
(**CycleGAN** [4] - **G**: Res-Net; **D**: PatchGAN)

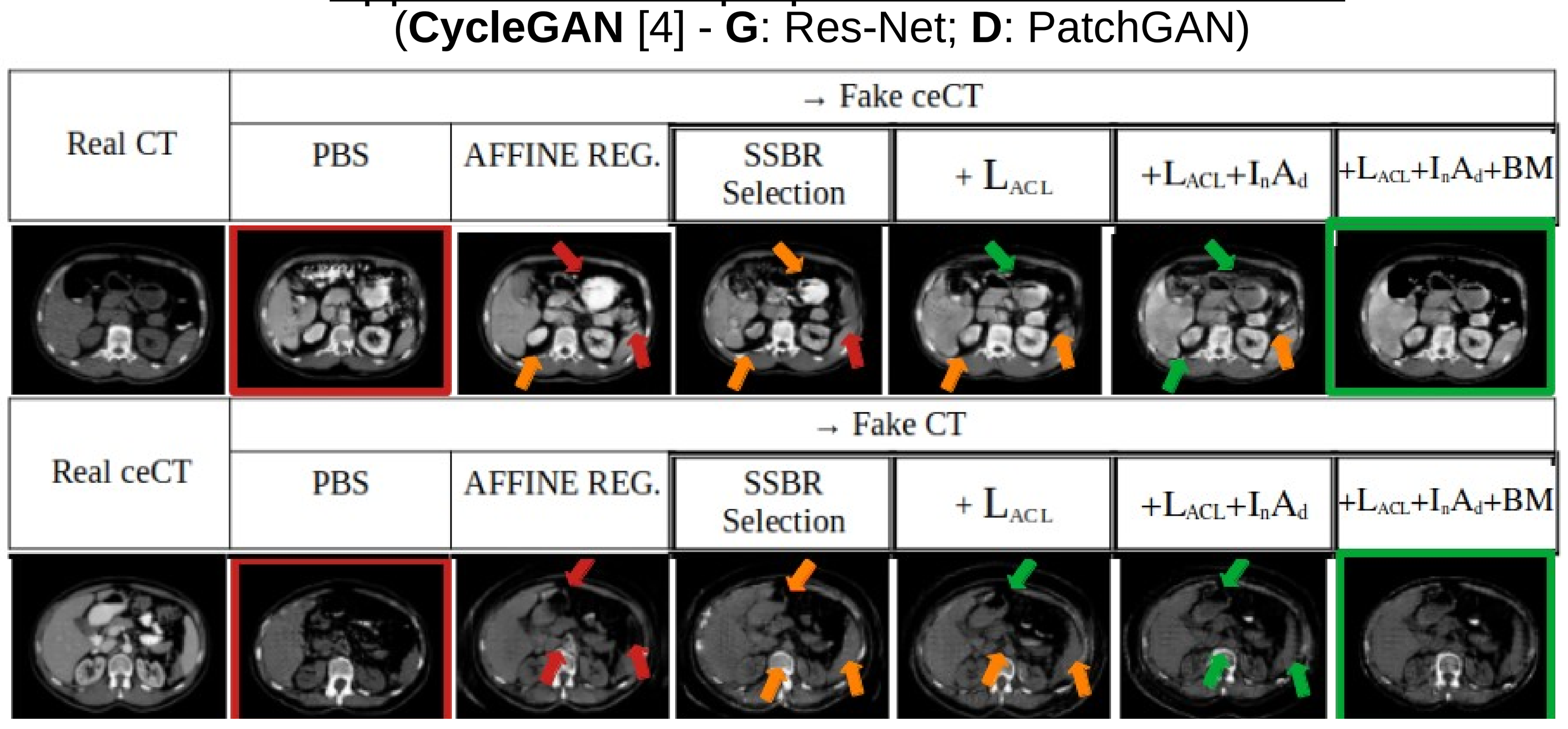

- **Quantitative study on paired database –** pediatric and pathological database of Necker hospital of 10 paired ceCT-CT images

Ablation study using pre-trained network on unpaired data

CycleGAN Method	MSE $[10^{-2}]$ (↓)	SSIM $[10^{-1}]$ (↑)	PSNR (↑)	TIME (↓)
real CT→fake ceCT vs real ceCT				
PBS	10,05 (2,89)	5,76 (0,65)	16,14 (1,15)	3h 2m
AFFINE REG.	8,16 (1,80)	6,36 (0,57)	16,99 (0,87)	16h 33m
SSBR selection	9,07 (2,39)	5,99 (0,71)	16,56 (1,07)	7h 5m
$+L_{ACL}$	8,55 (2,28)	6,19 (0,69)	16,82 (1,07)	7h 49m
$+BM$	8,42 (2,46)	6,24 (0,73)	16,91 (1,17)	7h 5m
$+I_nA_d$	6,79 (2,85)	6,60 (0,74)	17,97 (1,54)	7h 14m
$+L_{ACL}+BM$	8,19 (2,32)	6,36 (0,72)	17,02 (1,14)	7h 49m
$+L_{ACL}+I_nA_d$	6,41 (1,97)	6,67 (0,63)	18,11 (1,22)	7h 55m
$+L_{ACL}+I_nA_d+BM$	**6,37 (2,01)**	**6,81 (0,62)**	**18,14 (1,23)**	7h 55m
real ceCT→fake CT vs real CT				
PBS	8,26 (1,97)	5,36 (0,28)	16,96 (1,04)	3h 2m
AFFINE REG.	4,72 (0,95)	6,77 (0,37)	19,36 (0,93)	16h 33m
SSBR selection	7,15 (2,16)	5,68 (0,52)	17,64 (1,26)	7h 5m
$+L_{ACL}$	5,87 (1,73)	6,08 (0,22)	18,47 (1,12)	7h 49m
$+BM$	6,07 (1,28)	6,61 (0,65)	18,28 (0,99)	7h 5m
$+I_nA_d$	6,16 (1,15)	5,87 (0,23)	18,18 (0,79)	7h 14m
$+L_{ACL}+BM$	5,08 (0,85)	6,87 (0,52)	19,02 (0,74)	7h 49m
$+L_{ACL}+I_nA_d$	4,24 (0,86)	6,80 (0,37)	19,83 (0,92)	7h 55m
$+L_{ACL}+I_nA_d+BM$	**4,05 (0,83)**	**7,23 (0,53)**	**20,03 (0,92)**	7h 55m

Blood vessel segmentation with the Levae-One-Patient-Out method using 3D nnU-Net [9]

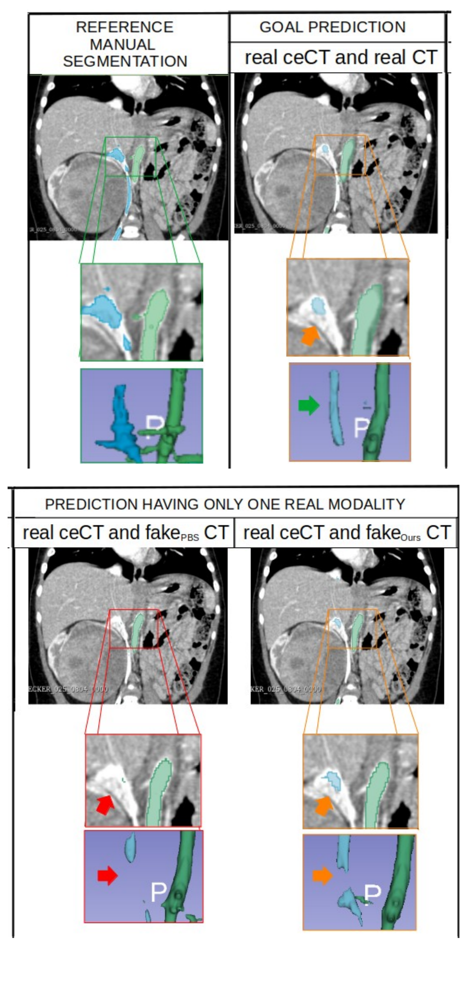

INPUT Database	Structure	DS [100%] (↑)	PR [100%] (↑)	RC [100%] (↑)	HD95 [mm] (↓)
on 10 patients					
real ceCT and real CT	Arteries	74.61 (5.89)	85.22 (8.32)	69.06 (8.15)	15.39 (5.72)
	Veins	45.62 (13.72)	60.61 (19.53)	38.68 (14.83)	31.47 (16.53)
real ceCT without data aug.	Arteries	63.75 (11.18)	80.33 (10.99)	53.88 (12.48)	23.43 (8.18)
	Veins	21.18 (19.70)	64.04 (34.08)	15.45 (16.04)	42.14 (23.79)
real ceCT	Arteries	73.01 (6.57)	81.08 (8.70)	67.19 (8.43)	15.80 (7.01)
	Veins	40.58 (23.50)	55.94 (31.39)	33.72 (26.61)	40.65 (30.90)
real ceCT and fake$_{PBS}$ CT	Arteries	69.59 (8.89)	79.54 (10.85)	63.47 (12.59)	18.08 (8.21)
	Veins	44.40 (22.75)	58.44 (21.78)	38.38 (23.20)	39.31 (16.79)
real ceCT and fake$_{Ours}$ CT	Arteries	**72.33 (7.41)**	77.29 (10.32)	68.63 (8.88)	**15.48 (6.38)**
	Veins	**44.49 (22.50)**	54.98 (26.74)	40.28 (22.69)	**38.90 (32.76)**
on 5 more heterogeneous					
real ceCT and real CT	Arteries	75.01 (5.82)	85.17 (4.37)	67.50 (8.57)	12.79 (6.04)
	Veins	40.87 (14.73)	56.93 (18.63)	32.62 (13.05)	31.16 (10.76)
real ceCT without data aug.	Arteries	66.59 (8.31)	86.89 (5.70)	54.83 (10.29)	23.34 (9.14)
	Veins	14.66 (17.05)	71.31 (39.90)	8.89 (10.98)	50.35 (29.50)
real ceCT	Arteries	72.94 (6.30)	84.37 (3.80)	64.89 (9.71)	13.49 (5.14)
	Veins	28.28 (19.84)	51.97 (38.06)	17.50 (18.41)	35.57 (14.33)
real ceCT and fake$_{PBS}$ CT	Arteries	70.77 (9.18)	84.41 (5.96)	63.00 (15.51)	13.83 (5.95)
	Veins	33.47 (26.92)	45.48 (34.33)	27.73 (23.78)	37.73 (23.42)
real ceCT and fake$_{Ours}$ CT	Arteries	**73.18 (7.51)**	80.58 (4.59)	67.63 (11.25)	**12.73 (4.10)**
	Veins	**40.57 (20.25)**	62.01 (13.31)	31.96 (18.91)	**32.83 (13.84)**

November 2022 BMVC

CONCLUSION

- We showed significant improvements in the generated images compared to existing methods.
- We demonstrated that the synthesized images can be used to guide a segmentation method by compensating, without loss of performance, for the absence of the complementary real acquisition modality.

[1] V Sandfort et al. (2019). [2] X Yi et al. (2019). [3] H Yang et al. (2020). [4] Y Zhu et al. (2017). [5] K Yan et al. (2018). [6] K Clark et al. (2013). [7] A Odena et al. (2017). [8] Y Jiang et al. (2021). [9] F Isensee et al. (2021).

Contact giammarco.labarbera@telecom-paris.fr

BMVC 2022 Communication ID **0776**